Materials Research Proceedings **26** (2023) 485-490 https://doi.org/10.21741/9781644902431-79

Static and dynamic response analysis of stay cables using terrestrial laser scanning and vibration measurements

Cecilia Rinaldi[1, a *], Marco Lepidi[2, b] and Vincenzo Gattulli[1,c]

[1]Dept. of Structural and Geotechnical Engineering, Sapienza University of Rome, Rome, Italy

[2]Dept. of Civil, Chemical and Environmental Engineering, University of Genova, Genova, Italy

[a]cecilia.rinaldi@uniroma1.it, [b]marco.lepidi@unige.it, [c]vincenzo.gattulli@uniroma1.it

Keywords: Inclined Suspended Cables, Modal Analysis, Point Cloud Model, Vision-Based Measurement, Cable Tension Estimation

Abstract. Nowadays, high accuracy measurements provided by terrestrial laser scanner and vision sensors allow to collect useful and exhaustive information about the conditions of the existing structures, useful to detect defects and geometry anomalies and to better understand their mechanical behavior. These avant-garde technologies were found to be particularly effective for the structural health assessment of the cable-stayed pedestrian bridge described in this paper. Considering a continuous mono-dimensional model of an inclined perfectly flexible cable, the axial tension is locally tangent to the cable profile. Thus, determining the cable static response under self-weight consists of a geometric shape-finding problem. Through terrestrial laser scanning, a 3D point cloud model of the bridge was acquired, including a data-abundant description of the actual static configuration of the stays. Therefore, cable configuration was no longer an unknown of the static problem, which can be inverted to assess the static tension. Furthermore, modal analysis was conducted also through image-based vibrations measurements to identify the fundamental frequencies of the cables. The independent identification of the axial forces from static (geometric) and dynamic (spectral) data provided results in good agreement.

Introduction

Structural cables are primary load bearing elements in different civil engineering systems, such as cable-stayed and suspension bridge. The assessment of their integrity condition and stress level are key tasks in the health monitoring of such structures. Among the techniques used to identity cable forces, direct methods make use of load sensors, while indirect methods estimate cable tension through different quantities such as strain, or natural frequencies [1],[2].

The dynamic identification method based on determining the unknown cable tension from the geometric stiffness that can be evaluated for measured frequencies (known the cable mass) is the most used, because it is a nondestructive method which guarantees high efficiency [3],[4],[5]. Similarly to other model based methods, this approach requires refined mechanical formulations describing the dependence of the spectral properties on the structural parameters [6],[7]. In addition to traditional accelerometer sensors, different technologies are used to record cable vibrations. Microwave interferometry has been used to measure the vibration response of cables in cable-stayed bridges [8],[9]. Frequencies and cable tensions have been identified through radar technique with the same accuracy of the ones obtained with conventional sensor measurements. Modal analysis and axial force identification of stay cables are also performed through vision-based measurement, with motion magnification methods used to amplify microvibration of stay cable captured by video camera [10]. If not based sufficiently refined mechanical methods, frequency-based approaches often neglect or underrate the effects of the chord inclination angle, cable extensibility, flexural stiffness, complex boundary conditions and cable-beam interactions. All these effects could lead to significant errors in tension identification.

Materials Research Proceedings **26** (2023) 485-490 https://doi.org/10.21741/9781644902431-79

In this work, the 3D point cloud model of a cable-stayed pedestrian bridge was exploited to evaluate the actual static configuration of the stays and to identify their axial forces by comparing the quadratic term coefficient of the cubic function interpolating the acquired geometry data with the quadratic term of the cubic equation obtained from an approximate solution of the static problem. The quality of the estimation of cable force was evaluated through the definition of an error function based on the cubic term the interpolating function and thorough the comparison with the tension identified through frequency-based method.

Bridge description and data acquisition

The bridge is a steel truss structure located in Beinasco, Turin province, in Italy. It is a cycle and pedestrian cable-stayed bridge and consists of an access ramp and a deck both supported by steel columns and cables anchored to a steel tubular pylon (see Fig. 1) with star reinforcements in 15 mm thick shaped sheets, hinged at the base. The deck (80 m long, 3 m wide and 1.65 m height) is made of three main tubular members and smaller cross-members and it is supported by 7 cables (42 mm diameter), all prestressed during assembly to avoid loosening. The first part of the access ramp is simply supported on columns while the second part is suspended by other stays (28 mm diameter) converging on the same pylon that supports the deck. Several cables (40 and 42 mm diameter) connect the pylon to the ground, to ensure stability and counterbalance the loads of the deck and ramp. On the side of the ramp, the steel truss-type beam of the deck is also supported by an access concrete staircase which is located at the center of the ramp.

Experimental data were acquired by different technologies to collect both geometry and vibration information of the structure. The terrestrial laser scanner Cam2 Laser Scanner Focus Faro x 130 (130 m unambiguity interval, 0.6 m - 130 m Range Focus3D X 130 HDR, 122000/244000/ 488000/976000 points/sec measurement speed, ±2 mm distance error) was used to acquire actual geometry configuration of the whole structure; during the scans, it acquired measurements by the appropriate laser and photographs in both color and black and white. The given color allowed to obtain three-dimensional RGB models (see Fig. 1b).

Wireless and wired accelerometers and a high-speed camera were used to record structural dynamic response under ambient excitation. The vibrations of the cables were recorded by using 6 uniaxial piezoelectric wired accelerometers, PCB 393B31 with ICP technology (10.0 V/g sensitivity, 0.5 g pk measurement range, 200 Hz sampling frequency). Furthermore, the high-speed camera IO Industries Flare 12M125xCL (monochrome, F-mount, 4096 x 3072 resolution, 5.5 x 5.5 µm pixel size, 100-200 fps sampling frequency) was installed on the concrete cantilever of the stairs located in the central area of the ramp to record the vibration of cables SP15 and SP16 (Fig. 4a). The displacement time histories were obtained by processing the captured images with Digital Image Correlation (DIC) technique.

a)  b) 

Fig. 1. Beinasco bridge: a) plan view of the cable-stayed; b) side view of the 3D point cloud model.

Cable tension identification from static configuration

Consider a suspended cable hanging on a vertical plane under self-weight. Let S be the set of N laser-scanned points belonging to the cable, pointed by the configuration vector $\mathbf{X}_i = (X_i, Y_i, Z_i)$,

Materials Research Proceedings **26** (2023) 485-490 https://doi.org/10.21741/9781644902431-79

within an orthogonal Cartesian reference system in a three-dimensional space (with $i = 1,...,N$). The vertical midplane of the N coordinate points is sought through the equations

$$y = ax + b\,, \quad a = \frac{1}{M}\sum a_{ij}\,, \quad b = \frac{1}{M}\sum b_{ij}\,, \tag{1}$$

where the coefficients a_{ij} and b_{ij} are determined by taking $M = N_r^2$ pairs of points (i, j) from the cable point cloud model, according to the formulas

$$a_{ij} = \frac{Y_i - Y_j}{X_i - X_j} = \frac{Y_j - Y_i}{X_j - X_i} = a_{ji}\,, \quad b_{ij} = \frac{X_i Y_j - X_j Y_i}{X_i - X_j} = \frac{X_j Y_i - X_i Y_j}{X_j - X_i} = b_{ji}\,, \tag{2}$$

where a subset of $2N_r < N$ points has been selected, namely N_r points $\mathbf{X}_i$ and N_r points $\mathbf{X}_j$ close to the lower and upper cable support – respectively – with the aim of maximizing the accuracy of the coefficient estimates by maximizing the denominators in equations (2). The coefficients a_{ij} and b_{ij}, obtained for each pair of points considered, are represented in the plane (a, b) in Fig. 2. It can be noted that the results associated to the same point $\mathbf{X}_i$ are approximately aligned. This behaviour can be easily justified by considering that, with respect to a fixed lower point $\mathbf{X}_i$, the positions of the upper points $\mathbf{X}_j$ (that are close to each other) determine small variations of the coefficients a_{ij} and b_{ij}, that can be estimated through their first variations

$$\delta a_{ij} = \frac{\partial a_{ij}(X_j, Y_j)}{\partial X_j}\delta X_j + \frac{\partial a_{ij}(X_j, Y_j)}{\partial Y_j}\delta Y_j\,, \quad \delta b_{ij} = \frac{\partial b_{ij}(X_j, Y_j)}{\partial X_j}\delta X_j + \frac{\partial a_{ij}(X_j, Y_j)}{\partial Y_j}\delta Y_j\,, \tag{3}$$

so that it can be demonstrated that the ratio $\delta b_{ij} / \delta a_{ij} = -X_i$ is a constant. The midplane identified with this procedure is represented in Fig. 2b. A roto-translation of the reference system are performed to make the Cartesian plane $\Pi(X, Z)$ coincident with the midplane of the cable.

The geometric curve to be identified based on the cable points is postulated to be describable by a cubic function $Z(X)$. Suited dimensionless variables and parameters are introduced

$$z = \frac{Z}{L}\,, \quad x = \frac{X}{L}\,, \quad \theta = \mathrm{arctg}\left(B/L\right), \tag{4}$$

where the lengths L and B are the horizontal and vertical distance between the supports of the cable (assumed known) and θ is the angle of the cable chord with respect to the horizontal.

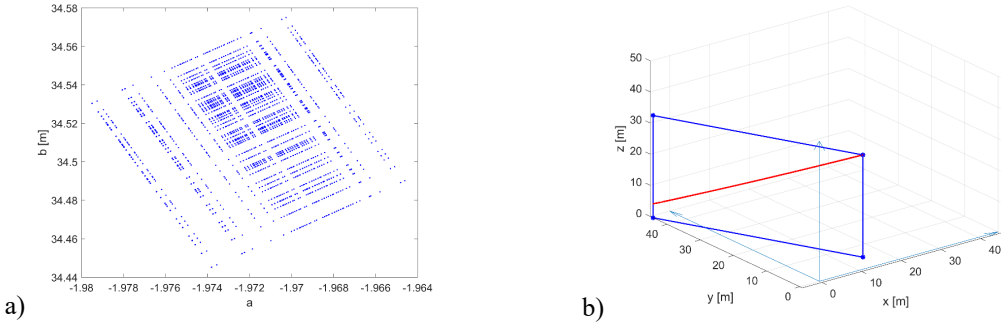

a) b)

Fig. 2. Midplane of the 3D point cloud of cable: a) coefficients a_{ij} and b_{ij}; b) vertical midplane identified (blue) and 3D point cloud model of the cable (red).

By employing nondimensional variables, the generic expression of the cubic function $z(x)$ depends on four unknown coefficients γ_i, according to the formula

$$z(x) = \gamma_0 x^3 + \gamma_1 x^2 + \gamma_2 x + \gamma_3\,. \tag{5}$$

Therefore, by imposing the geometric boundary conditions $z(x)_{x=0} = 0$ and $z(x)_{x=1} = -\tan\theta$, the cubic expression becomes

Materials Research Proceedings **26** (2023) 485-490 https://doi.org/10.21741/9781644902431-79

$$z(x) = \gamma_0 x^3 + \gamma_1 x^2 - (\gamma_1 + \gamma_0 + \tan\theta)x\,, \tag{6}$$

where the coefficients γ_0 and γ_1 are unknown, but univocally determinable for each pair of laser-scanned points $\mathbf{x}_1 = (x_1, z_1)$ and $\mathbf{x}_2 = (x_2, z_2)$ lying on the midplane through the formulas

$$\gamma_0 = \frac{x_1 z_2 (1-x_1) - x_2 z_1 (1-x_2) - \Delta(x_1, x_2)}{x_1 x_2 (1-x_1)(1-x_2)(x_1 - x_2)}, \qquad \gamma_1 = \frac{x_2 z_1 (1-x_2^2) - x_1 z_2 (1-x_1^2) + (x_1 + x_2)\Delta(x_1 x_2)}{x_1 x_2 (1-x_1)(1-x_2)(x_1 - x_2)}, \tag{7}$$

where $\Delta(x_1, x_2) = x_1 x_2 (x_1 - x_2)\tan\theta$. A subset of $2N_s < N$ points has been selected, namely N_s points $\mathbf{x}_1$ and N_s points $\mathbf{x}_2$ close to the lower and upper thirds of the cable profile, respectively, with the aim of maximizing the accuracy of the coefficient estimates by maximizing the denominators in equations (7). The coefficients γ_0 and γ_1, obtained for each pair of points considered, are represented in the plane (γ_0, γ_1) in Fig. 3. Again, the alignments of the results can be justified by considering that, with respect to a fixed lower third point $\mathbf{x}_1$, the positions of the upper third points $\mathbf{x}_2$ (that are close to each other) determine small variations of the coefficients γ_0 and γ_1, and that the ratio of the first variations is $\delta\gamma_1 / \delta\gamma_0 = -(x_1 + 1)$ is constant.

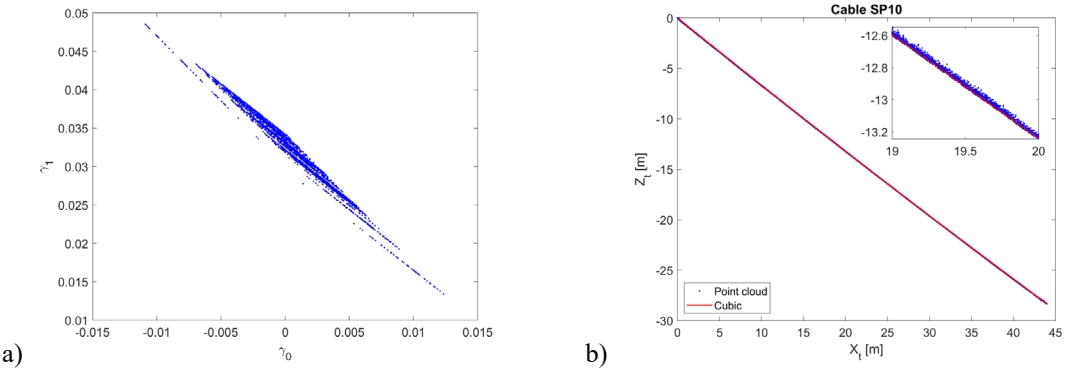

Fig. 3. Geometric interpolation of cable axis: a) coefficients of cubic function, b) overlap of the cubic interpolation with the point cloud model.

The *nonlinear* ordinary differential equation governing the static equilibrium under self-weight of the inextensible cable, considering constant weight per unit natural length w, reads

$$z'' = -8\delta\cos\theta\left[1 + (z')^2\right]^{1/2}, \qquad \text{with} \quad \delta = (wL)/(8H\cos\theta)\,, \tag{8}$$

where H is the unknown horizontal reaction. It is known that this equation admits the catenary function as exact solution. Since the catenary solution can be difficult to handle, equation (8) can be attacked employing a classic perturbation scheme. Setting the parameter and variable ordering

$$\delta = \varepsilon\delta_1\,, \qquad \tilde{z}(x) = \varepsilon\tilde{z}_1(x) + \varepsilon^2\tilde{z}_2(x) + \varepsilon^3\tilde{z}_3(x) + \ldots \tag{9}$$

where $\tilde{z}(x) = z(x) - x\tan\theta$ describes the depth of the cable with respect to the chord and $\varepsilon << 1$ is a small auxiliary nondimensional parameter with mere bookkeeping role.

From the physical viewpoint, it is important to note that the ordering entails that the cable weight-to-tension ratio is small ($\delta = O(\varepsilon)$) and the depth of the cable is shallow ($\tilde{z}(x) = O(\varepsilon)$). Introducing the ordering in equation (8), expanding in ε-power series, collecting same-order terms and solving the resulting ordered hierarchy of *linear* ordinary differential equations up to the second order with the boundary conditions $\tilde{z}_i(0) = 0$ and $\tilde{z}_i(1) = 0$, the solutions are

$$\tilde{z}_1 = 4\delta_1 x(1-x)\,, \quad \tilde{z}_2 = \tfrac{8}{3}\delta_1^2 \sin(2\theta)x(1-x)(1-2x)\,. \tag{10}$$

After reconstruction, the direct comparison of the cubic function (5) and the cubic perturbation solution $z(x) = \tilde{z}(x) + tan\,\theta \simeq tan\,\theta + \varepsilon\tilde{z}_1(x) + \varepsilon^2\tilde{z}_2(x)$ allows to identify the unknown parameter δ by equating the respective quadratic and cubic coefficients. To circumvent the redundancy, the identification can be based on the quadratic coefficient γ_1, being larger. The equality reads

$$4\delta(1+2\delta\sin(2\theta)) = \gamma_1 \tag{11}$$

and establishes a quadratic equation in the unknown δ, that must be solved for positive values δ_*. The comparison between cubic coefficients, being smaller, can provide an estimate of the identification inaccuracy $\delta_e = -\gamma_0 - \frac{16}{3}\delta_*^2 \sin(2\theta)$. Once the parameter δ is determined, the horizontal reaction H and the cable tension $N \simeq \frac{H}{cos\,\theta}$ can be assessed by inverting the parameter definition, provided that the cable weight w is known. The mean values (and their variance) obtained with this approach are listed in Tab.1 for seven stays of the Beinasco bridge.

Frequency-based cable axial force identification

The small-amplitude free oscillations of the bridge stays have been investigated according to the linearized undamped dynamics of suspended cables. According to the Irvine cable model [11], [12], which is based on assuming parabolic static profile, linear elastic behavior and negligible longitudinal inertia, the cable axial force can be identified by employing the circular frequency ω_j of j-th out-of-plane modes, according to the direct and inverse (string-like) relations

$$\omega_j = \frac{j\pi\cos\theta}{L}\sqrt{\frac{N}{m}}\,, \qquad N = \frac{m\omega_j^2 L^2}{j^2\pi^2\cos^2\theta}\,, \tag{12}$$

where *m* the uniformly distributed mass density. Accordingly, the j-th frequency is expected to be directly and linearly related to the out-of-plane mode number j in the peak-picking frequency identification based on the Power Spectral Density (PSD) of the experimental signals. Such linear relation is clearly noticeable in the PSD of the camera signal, more than the accelerometer one (Fig. 4), because camera signals allow to identify the fundamental frequencies of the cables, which appeared to be lower than 1 Hz. The mean values (and their variance) obtained with this tension identification approach are listed in Tab. 1 for seven stays of the Beinasco bridge.

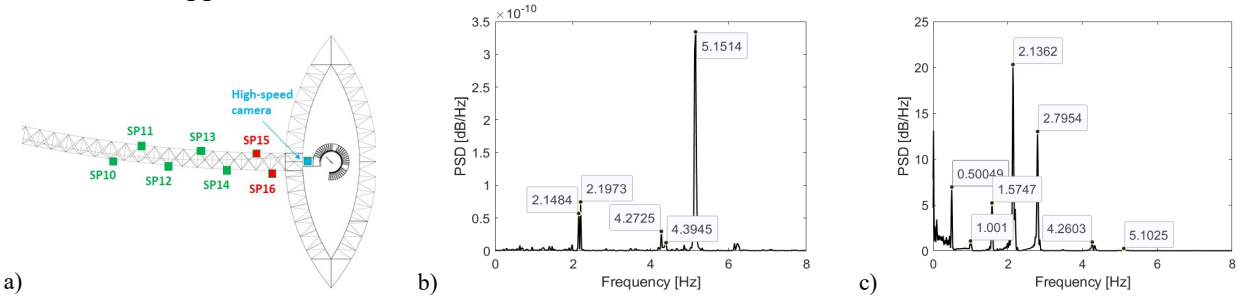

a) b) c)

Fig. 4. Frequency identification of cable SP15: a) plan view of cable and camera position; b) PSD of accelerometer signals, c) PSD of image-based displacement signal.

Concluding remarks

The paper investigates the static and dynamic response of the stays supporting a cable-stayed pedestrian bridge, by exploiting experimental data concerning both geometry configuration and vibration response to ambient excitation. By referring to a continuous perfectly flexible model of inclined suspended cable, and by considering the laser-scanned geometry of the stays, the static configuration under self-weight has been consistently described. This description allowed the

static (geometry-based) identification of the cable tension, which has resulted in good agreement with the tensions evaluated through the dynamic (frequency-based) output-only identification method, applied to both accelerometer and image-based vibration signals.

Tab. 1. Cable tension from static identification N_s and from dynamic identification N_d.

Cable	γ_0	$\sigma^2_{\gamma_0}$	γ_1	$\sigma^2_{\gamma_1}$	θ	δ_*	$\sigma^2_{\delta_*}$	δ_e	$\sigma^2_{\delta_e}$	N_s [kN]	N_d [kN]
SP10	4.84E-04	1.09E-05	3.22E-02	2.63E-05	0.57	7.94E-03	1.56E-06	-7.91E-04	1.02E-05	97.19	94.89
SP11	-7.35E-03	2.41E-05	5.12E-02	4.64E-05	0.65	1.25E-02	2.63E-06	6.55E-03	2.20E-05	59.39	58.78
SP12	1.35E-02	4.21E-05	1.22E-01	8.32E-05	0.73	2.89E-02	4.18E-06	-1.79E-02	3.44E-05	26.19	26.02
SP13	-3.50E-03	8.55E-05	1.75E-01	1.87E-04	0.83	4.05E-02	8.67E-06	-5.21E-03	6.36E-05	18.39	19.54
SP14	-9.73E-04	2.77E-04	6.14E-02	6.48E-04	0.94	1.49E-02	3.60E-05	-1.56E-04	2.45E-04	54.25	41.68
SP15	-2.06E-02	1.91E-04	2.49E-01	4.68E-04	1.04	5.67E-02	2.01E-05	5.59E-03	1.30E-04	16.32	17.83
SP16	2.95E-02	7.65E-04	7.59E-02	2.12E-03	1.11	1.84E-02	1.15E-04	-3.10E-02	6.58E-04	53.78	44.31

Acknowledgments
This research was in part sponsored by the NATO Science for Peace and Security Programme under grant id. G5924.

References
[1] A.B. Mehrabi, "In-service evaluation of cable-stayed bridges, overview of available methods and findings" *Journal of Bridge Engineering* 11(6), pp. 716–724, 2006. https://doi.org/10.1061/(ASCE)1084-0702(2006)11:6(716)
[2] L. Zhang, G. Qiu, Z. Chen, "Structural health monitoring methods of cables in cable-stayed bridge: A review" *Measurement* 168, id.108343, 2021. https://doi.org/10.1016/j.measurement.2020.108343
[3] M. Lepidi, V. Gattulli, F, Vestroni, F. "Damage identification in elastic suspended cables through frequency measurement" *Journal of Vibration and Control* 15(6), pp.867-896, 2009. https://doi.org/10.1177/1077546308096107
[4] S. Jeong, H. Kim, J. Lee, S.-H. Sim, "Automated wireless monitoring system for cable tension forces using deep learning" *Structural Health Monitoring* 20(4), pp. 1805-1821, 2021. https://doi.org/10.1177/1475921720935837
[5] S.-W. Kim, J.-H. Cheung, J.-B. Park, S.-O. Na, "Image-based back analysis for tension estimation of suspension bridge hanger cables" *Structural Control and Health Monitoring* 27(4), id.e2508, 2020. https://doi.org/10.1002/stc.2508
[6] V. Gattulli, M. Lepidi, F. Potenza, U. Di Sabatino, "Modal interactions in the nonlinear dynamics of a beam-cable-beam" *Nonlinear dynamics* 96(4), pp.2547-2566, 2019. https://doi.org/10.1007/s11071-019-04940-8
[7] V. Gattulli, M. Lepidi, F. Potenza, U. Di Sabatino, "Dynamics of masonry walls connected by a vibrating cable in a historic structure" *Meccanica* 51(11), pp. 2813-2826, 2016. https://doi.org/10.1007/s11012-016-0509-9
[8] C. Gentile, "Deflection measurement on vibrating stay cables by non-contact microwave inter-ferometer" *Ndt & E International* 43(3), pp. 231-240, 2010. https://doi.org/10.1016/j.ndteint.2009.11.007
[9] C. Gentile A. Cabboi, "Vibration-based structural health monitoring of stay cables by microwave remote sensing" *Smart Structures and Systems* 16(2), pp. 263-280, 2015. https://doi.org/10.12989/sss.2015.16.2.263
[10] S. Wangchuk, D.M. Siringoringo, Y. Fujino, "Modal analysis and tension estimation of stay cables using noncontact vision-based motion magnification method" *Structural Control and Health Monitoring* 29(7), id. e2957, 2022. https://doi.org/10.1002/stc.2957
[11] H. M. Irvine, Cable Structures. The MIT Press, 1981.
[12] M. Lepidi V. Gattulli, "Static and dynamic response of elastic suspended cables with thermal effects" *International Journal of Solids and Structures* 49(9), pp. 1103-1116, 2012. https://doi.org/10.1016/j.ijsolstr.2012.01.008

Materials Research Proceedings **26** (2023) 485-490 https://doi.org/10.21741/9781644902431-79